Journal of Power Sources 189 (2009) 1106–1113

Contents lists available at ScienceDirect

Journal of Power Sources

journal homepage: www.elsevier.com/locate/jpowsour

The performance of solid oxide fuel cells with Mn–Co electroplated interconnect as cathode current collector

Junwei Wu [a,b], Christopher D. Johnson [a], Randall S. Gemmen [a], Xingbo Liu [a,b,*]

[a] National Energy Technology Laboratory, Department of Energy, Morgantown, WV 26507, USA
[b] Mechanical and Aerospace Engineering Department, West Virginia University, Morgantown, WV 26506, USA

ARTICLE INFO

Article history:
Received 4 December 2008
Received in revised form 17 December 2008
Accepted 17 December 2008
Available online 30 December 2008

Keywords:
On-cell test
SOFC
Interconnect
Spinel
Electroplating

ABSTRACT

To add a coating on a metallic interconnect is one option to prevent Cr poisoning of the cathode and to retain high conductivity during solid oxide fuel cells (SOFC) operation. Electroplating of metals or alloys followed by oxidation offers a cost-effective method. In this study, pure Co and Mn/Co alloys formed by electrodeposition are used to protect the substrate, SUS 430. On-cell tests, using uncoated, cobalt-coated and MnCo-coated interconnects were conducted at 375 mA cm^{-2} for 323, 500 and 820 h, respectively. The results show that cell power degrades at a rate of 33% in 320 h using an uncoated interconnect. Significant improvements are obtained for cell tests utilizing unoptimized coated interconnects with the degradation rate of 5% and 9% per 1000 h for cobalt and MnCo coatings, respectively. Based on the results from SEM and XRD studies, the advantages of both coatings are to successfully inhibit Cr diffusion to the scale surface. However, thin (~2 μm) cobalt coating allows fast scale growth, while thicker cobalt coatings have the potential to fail due to mismatch in the coefficient of temperature expansion (CTE) between Co_3O_4 and the SUS 430 substrate. In spite of higher degradation rate for the MnCo coatings evaluated here, the addition of Mn into the cobalt coating not only aids in suppression of scale growth, but also reduces the CTE mismatch. Furthermore, no performance decay after two thermal cycles was observed. Finally, the cell degradation was observed to have a correlation with the cell cathode interlayer microstructure.

1. Introduction

With the reduction of solid oxide fuel cells (SOFC) operation temperatures to 800 °C, it is possible to use metallic interconnect materials as interconnects to replace the ceramic, $LaCrO_3$, which has been commonly used for ca. 950–1000 °C technology [1,2]. Ferritic stainless steels, chromia-formation alloys, are among the most promising alloys given that their coefficient of temperature expansion (CTE) is close to that of others SOFC ceramic components [3,4]. However, oxidation resistance is limited in these alloys. Excessive growth of chromia and chromium evaporation into the cathode can increase the cell resistance and polarization resistance significantly [5]. Although chromium-tolerant cathodes [6] and modified low Cr alloy [7] have been reported, an effective surface coatings is a viable approach, provided the coating cost is acceptably low. Single metal [8,9], perovskite [10,11], spinel [12,13] coated and Ce-treated [14] ferritic stainless steels have been reported previously, and some show acceptably low interconnect area specific resistances (ASR) after long term tests, but the Cr blockage capability is still uncertain for some of the coatings.

Among all of the possible coatings, $(Mn,Co)_3O_4$ spinel is one of the most promising due to its high conductivity, good chromium retention capability and good CTE match with the ferritic stainless steel substrate [12,15]. Thus far, slurry coating, screen-printing, and physical vapor deposition [16] have been applied to deposit these coatings. Electroplating of alloys followed by oxidation offers a cost-effective method to produce the desired spinels [17,18]. In our previous work, DC [19] and pulse plating [20] have been used to deposit Mn/Co alloy coatings. The ASR for the coated samples remains nearly stable over 1200 h, and no detectable Cr migrated to the top surface.

ASR tests have been used extensively to evaluate the effectiveness of interconnect coatings. Interconnects with a half cell (electrolyte and cathode) have been used to study the Cr poisoning mechanisms and the Cr tolerant cathode by Jiang and co-workers [21,6]. The advantages of fuel cell tests with interconnect are obvious, since such experiments can test both the resistance change and Cr poisoning effect simultaneously. However, very few studies [14,22–24] have reported the cell performance with direct contact interconnect materials. In this work, the main objectives are: (1)

* Corresponding author. Tel.: +1 304 293 3111x2324; fax: +1 304 293 6689.
E-mail address: xingbo.liu@mail.wvu.edu (X. Liu).

0378-7753/$ – see front matter © 2008 Elsevier B.V. All rights reserved.
doi:10.1016/j.jpowsour.2008.12.079

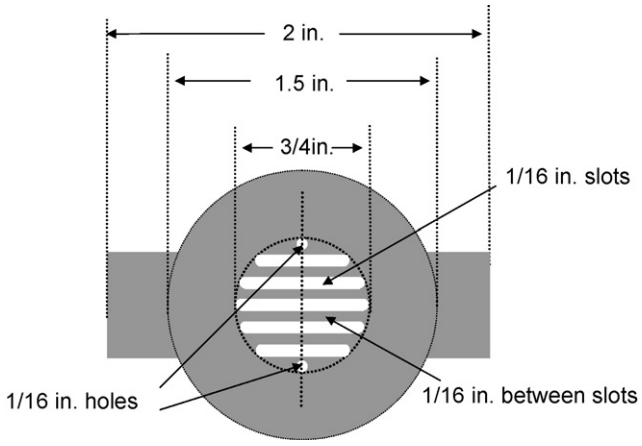

Fig. 1. Schematic presentation of the button cell interconnect.

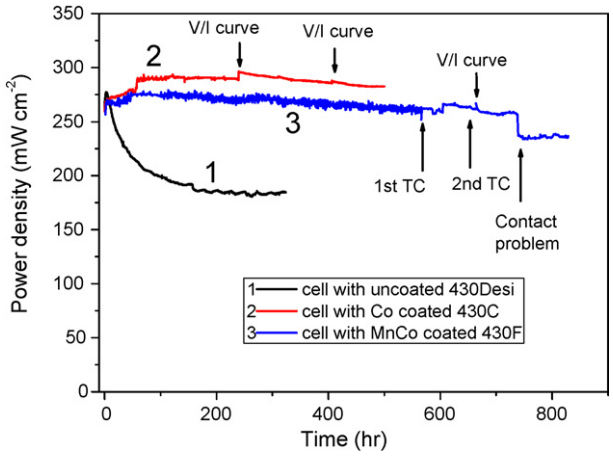

Fig. 3. Cell performances with interconnects as cathode current collectors.

to evaluate the performance of Co and MnCo-coated interconnects during long-term on-cell tests, as compared to the uncoated interconnect material, and (2) to investigate the detailed mechanisms of scale formation on these coated interconnects under real SOFC working conditions.

2. Experimental procedures

2.1. Interconnect and coating process

Ferritic stainless steel, SUS 430, was used as the substrate for the present work. One steel sample was a de-siliconized commercial alloy, supplied by Allegheny Ludlum with the silicon level ~0.2 wt%, and was used for the uncoated interconnect test. The other two interconnects were specially made at NETL Albany, with low levels of silicon and aluminum impurities (0.024 and 0.011 wt%, respectively), and were used for the coating tests.

The schematic of SOFC button cell current collector design is displayed in Fig. 1. All coupons were finished using 600# silica sandpaper before electrodeposition, then cleaned ultrasonically in acetone and then de-ionized water. The electrolytes used for pure Co plating in this experiment were prepared from solutions containing 0.1 M $CoSO_4$, and 6 g L^{-1} saccharin [23]. For Mn/Co co-deposition, the solution contained 0.10 M $CoSO_4$, 0.50 M $MnSO_4$, 0.70 M sodium gluconate, 1.0 M H_3BO_3, 0.10 M $(NH_4)_2SO_4$ [20]. The pulse electrodeposition parameters are 200 mA cm^{-2}, with 10ms on time and 5 ms off time. Total deposition period is 10 min.

The uncoated interconnect was prepared for testing simply by being grinded with 600# grit sandpaper and cleaned ultrasonically in acetone and then DI water. Oxidation of the coated samples was done for 2 h at 800 °C in air prior to testing.

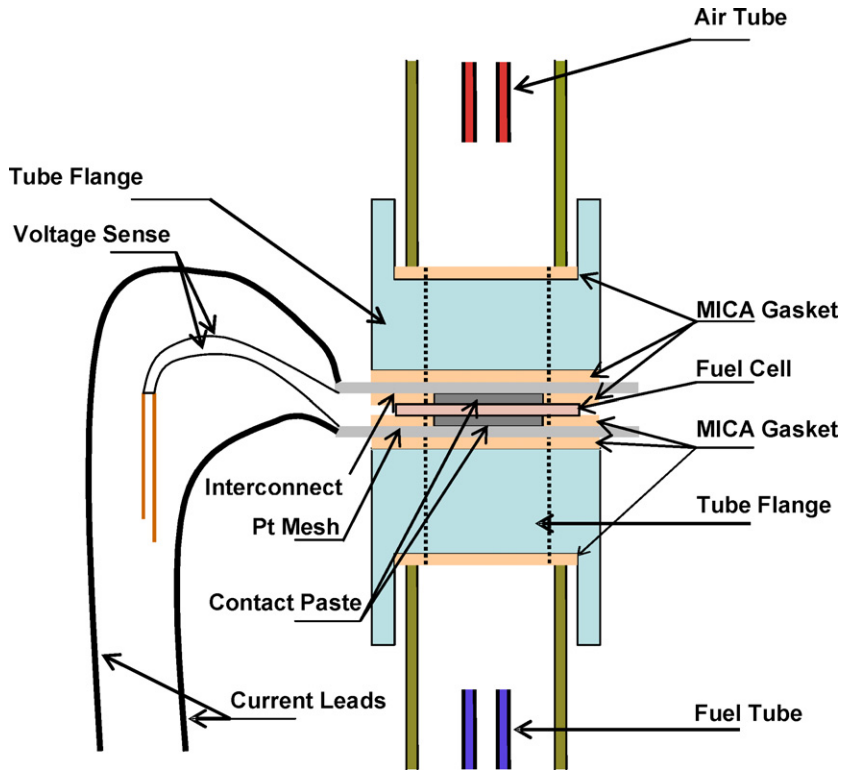

Fig. 2. Detailed cell test fixture.

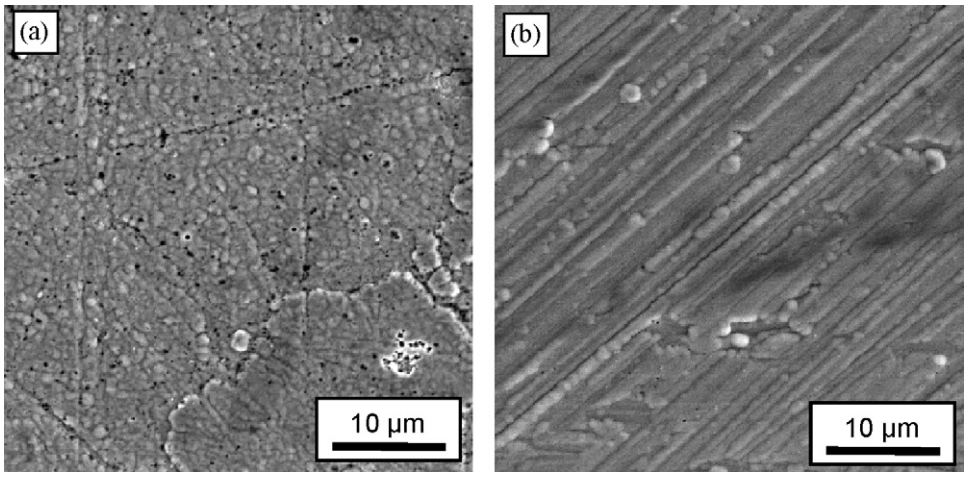

Fig. 4. As-deposited cobalt and MnCo coating on SUS 430 substrate. (a) Cobalt coating and (b) MnCo coating.

2.2. On-cell test

Fig. 2 shows the button cell test fixture used in this test. The interconnect was put on top of a platinum 10% rhodium mesh (0.003" wire diameter, UNIQUE wire weaving Co.), which in turn lay on top of the button cell cathode side. The anode side current collector consisted of platinum mesh, with Pt paint from SPI, Inc., used as a glue to maintain contact. A pure unhydrated mica sheet was used as the sealing material. All of the cells were anode-supported SOFCs from MSRI. The anode is a Ni/YSZ cermet, the electrolyte is yttria-stabilized zirconia (YSZ), and the cathode is lanthanum strontium manganate (LSM). An interlayer made of a finer grain mixture of LSM and YSZ is between the LSM and the YSZ electrolyte layers.

SOFCs were tested at 800 °C. After establishing initial cell open-circuit voltage (OCV), the oxidant flow rate was set at 500 cm^3 min^{-1} (97% air and 3% H_2O) and the fuel flow rate set at 100 cm^3 min^{-1} (97% H_2 + 3% H_2O). The cells were operated at a constant current level of 0.75 A (375 mA cm^{-2} relative to the cathode area). More details of the cell testing process have been previously published [14]. Periodically, the cells were subjected to voltage sweeps from 1.1 to 0.35 V to determine maximum power density. Before and after its use in the on-cell test, the Co-coated interconnect was subjected to thermal cycles to room temperature and back to 800 °C to test the adherence of the scale layer. During the on-cell test using the MnCo-coated interconnect, power loss led to an inadvertent thermal cycle to room temperature.

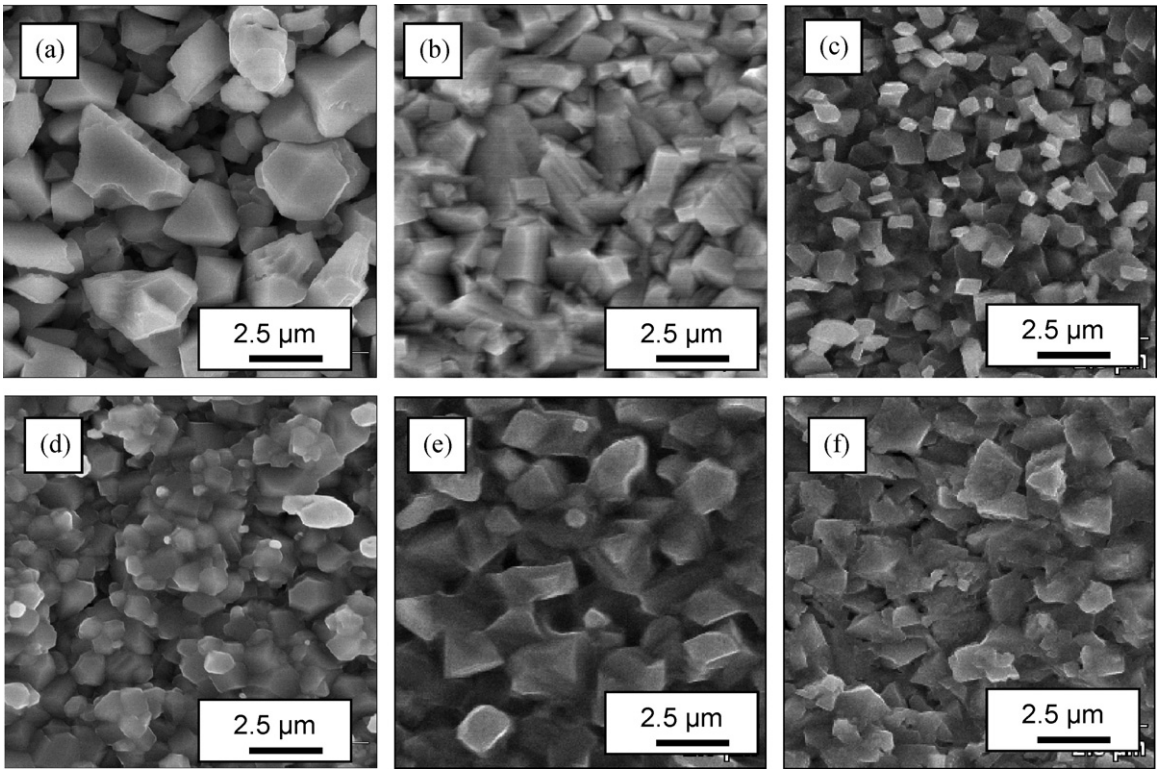

Fig. 5. SEM surface morphology of interconnect after on-cell test. (a and d) Un-contacted and contacted areas of the uncoated interconnect after 323 h test. (b and e) Un-contacted and contacted areas of Co-coated SUS 430 after 500 h test. (c and f) Un-contacted and contacted areas of MnCo-coated SUS 430 after 820 h test.

Table 1
EDX results of 15 kV for tested interconnect at 800 °C (at.%).

			O	Cr	Mn	Fe	Co
Uncoated (323 h)	Contacted	Fig. 4(a)	38	31	28	3	–
	Un-contacted	Fig. 4(d)	30	49	19	2	–
Co coated (500 h)	Contacted	Fig. 4(b)	28	3	9	20	39
	Un-contacted	Fig. 4(e)	29	2	4	13	52
MnCo-coated (820 h)	Contacted	Fig. 4(c)	30	7	12	9	42
	Un-contacted	Fig. 4(f)	32	2	7	6	53

Note: The time in the parenthesis is the interconnects on cell test period with applied load.

2.3. Interconnect and cell characterization

After the test, the surface morphology and composition of the coatings were assessed by a JEOL JSM 6300 FE-SEM equipped with a Thermo Electron EDS system. To characterize the phase formation, X-ray diffraction (XRD) data were obtained on a Panalytical MRD diffractometer equipped with a thin film stage. Additionally, interconnect and cell cross sections were also tested by SEM/EDX to study the element diffusion and Cr evaporation.

3. Results

3.1. Cell performance

Fig. 3 shows the cell performance variation with time at a constant current of 375 mA cm^{-2}. All of cells show similar power densities at the beginning of the long-term tests, but different trends are evident. The cell with the uncoated interconnect was tested for 323 h. It shows slight improvement in the initial 3 h. The power then degrades rapidly during the following 100 h, and then

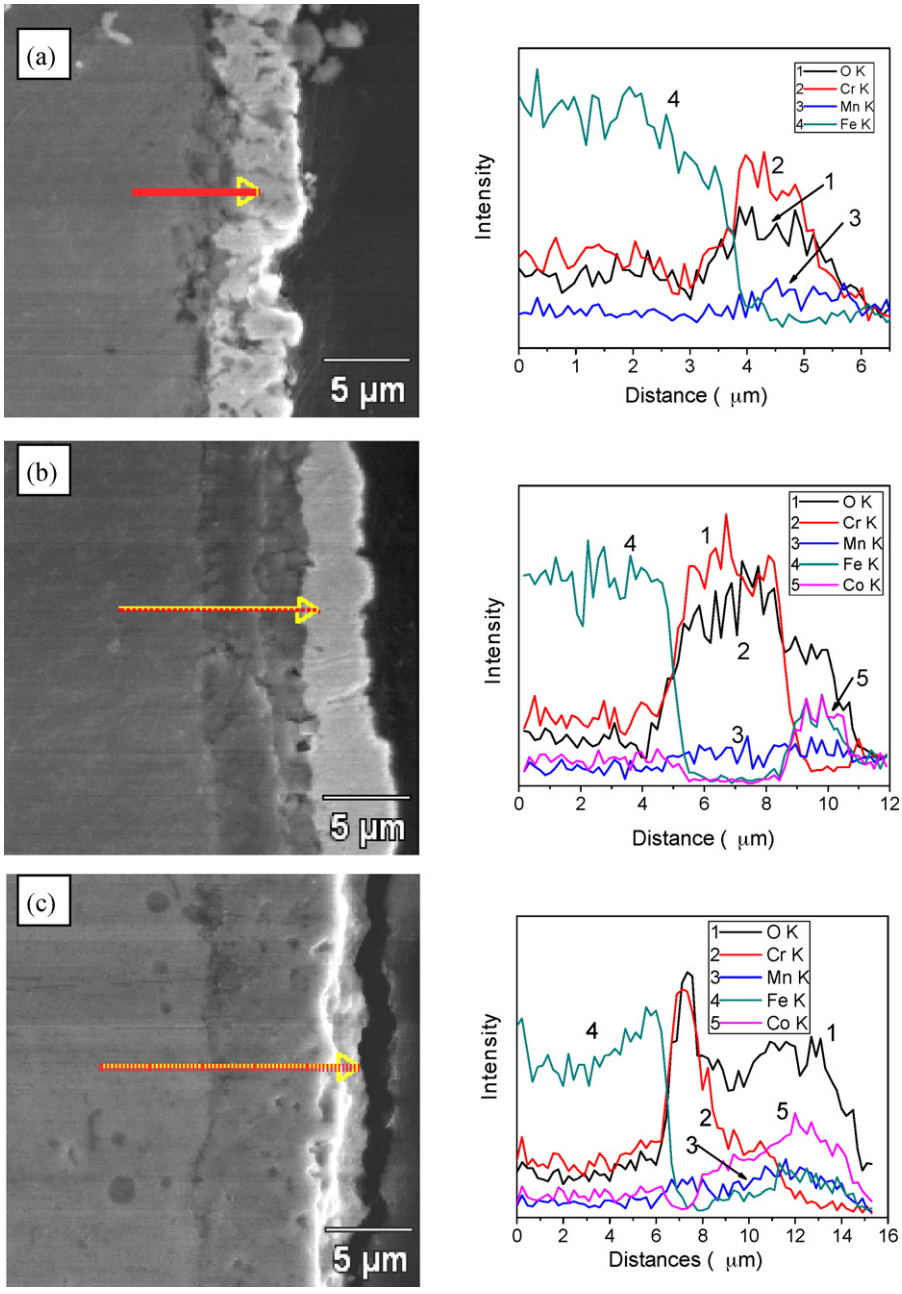

Fig. 6. Cross section SEM imaging and an EDS line scan of tested interconnect. The left side is substrate, and the right side bright layers are Pt paste at (a) and (b). (a) Uncoated interconnect after 323 h test. (b) Co-coated SUS 430 after 500 h test. (c) MnCo-coated SUS 430 after 820 h test.

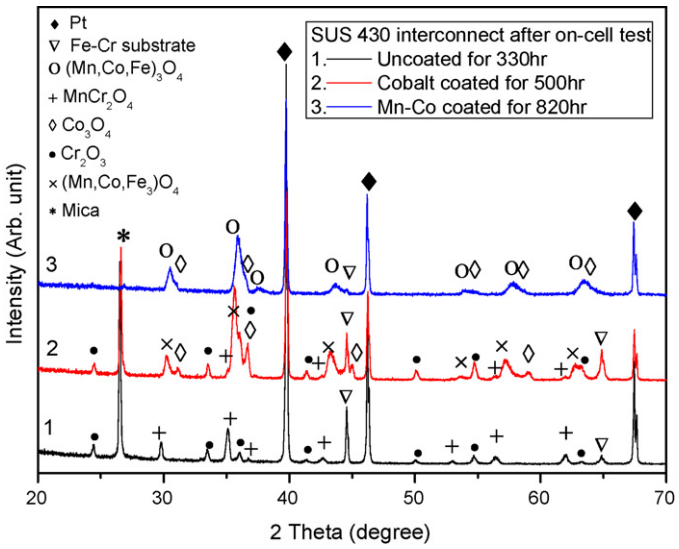

Fig. 7. XRD results of tested interconnect.

slows down and reaches a plateau at ~200 h. No thermal cycle is conducted during the cell test. Compared with highest power density of 277 mW cm^{-2}, the total degradation rate is 33% in the initial 200 h.

For the other two cells with coated interconnects, the power densities increase initially and reach maximum after about 60 h. The cell performance shows discontinuities that coincide with voltage/current curves measurement (V/I curves). The polarization curve results are not shown here. For the cell with the cobalt-coated interconnect, the maximum power density at 60 h is 290 and 283 mW cm^{-2} at 500 h. The rate of degradation is estimated as 5% per 1000 h. This interconnect was exposed to three thermal cycles prior to the on-cell test and two thermal cycles after test between room temperature and 800 °C. No spallation or any non-uniformity was observed after testing.

The cell tested with the MnCo-coated interconnect showed slight degradation from 50 to 735 h. At 735 h, the voltage suddenly dropped. This sudden decrease in cell voltage is believed to be the result of a voltage lead problem. In addition, at 566 and 650 h, two thermal cycles occured unintentionally at the same cell. After each thermal cycle, no performance drop was observed, suggesting that the MnCo coating adheres well to the steel substrate. The power density at 50 h is 275 and 258 mW cm^{-2} at 735 h. The estimated degradation rate is 9% per 1000 h.

3.2. Surface morphologies and compositions

Surface morphologies of the deposited interconnect coatings prior to air oxidation are displayed in Fig. 4. No obvious porosity is observed on the surface. The Co coating is uniform over the entire surface. The MnCo morphology shows the coating growth along the scratches created by polishing. EDX test shows tiny substrate peaks of iron and chromium at 15 kV (5 at.% and 2 at.% Fe for the cobalt and MnCo coating, respectively). Approximately 6 at.% Mn was incorporated into the MnCo coating.

Fig. 5 displays the surface morphologies of interconnects after the on-cell tests. Two images are shown: contacted areas and un-contacted areas (with the SOFC cathode). Un-contacted surfaces (Fig. 5(a), (b) and (c)) show cubic or diamond-like particles on the surface, which are typical spinel structures. Surfaces in contact with the cathode display all cubic particles connected to each other to form clusters.

Table 1 displays EDX (at 15 kV) results from Fig. 5. These data are considered to be mainly from the spinel layer and the chromia scale underneath the spinel layer. For the uncoated interconnect, the contact area has a higher content of Mn and Fe, and a lower content of Cr. Since the uncoated surface is mainly composed of chromia, these results imply an enhanced diffusion of Mn and Fe in the contact area. For the Co and MnCo-coated interconnects, all of the Mn, Fe and Cr contents are higher in the contacted area than in the un-contacted area. Cox et al. [25] reported that diffusivities of metal ions in Cr_2O_3 may decrease in the order $D_{Mn} > D_{Fe} > D_{Ni} > D_{Cr}$ by assuming that the metals diffuse as ions via Cr^{3+}-lattice sites in Cr_2O_3. Based on the data in Table 1, with current flow, element diffusion enhancement still roughly follows the order proposed by Cox et al. [25].

3.3. Coating cross section and EDX line scan

Fig. 6 shows SEM images and EDX line scans along the cross sections of the interconnects. All of them are from areas in contact with the fuel cell cathode. It is clear that bright layers, platinum paste layer, are spotted on the top of the coating or scale surface (Fig. 6(a) and (b)). For uncoated SUS 430, only Mn and Cr are detected between the substrate and Pt paste layer. The total scale layer is ~2 μm. It is obvious that three layers can be distinguished for both cobalt and MnCo-coated interconnects: coating, scale layer, and substrate. The cobalt-coated one shows a ~2 μm coating layer and ~3 μm scale layer. For the MnCo-coated interconnect, a total ~8 μm layer is observed on the top of the SUS 430 substrate. Only ~1 μm is a scale layer, and all other layers are cobalt containing spinels where the top layer is $(Mn,Co,Fe)_3O_4$ spinel. Note between

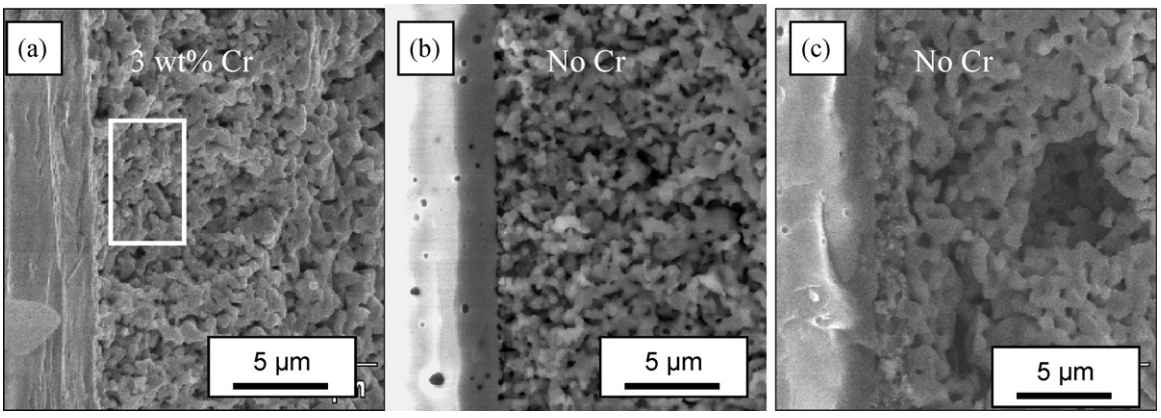

Fig. 8. Tested SOFC cathode cross sections. The left bright and gray regions are dense YSZ electrolyte, the right side is the bulk LSM cathode, and middle layers are LSM/YSZ interlay. (a) Uncoated interconnect after 323 h test. (b) Co-coated SUS 430 after 500 h test. (c) MnCo-coated SUS 430 after 820 h test.

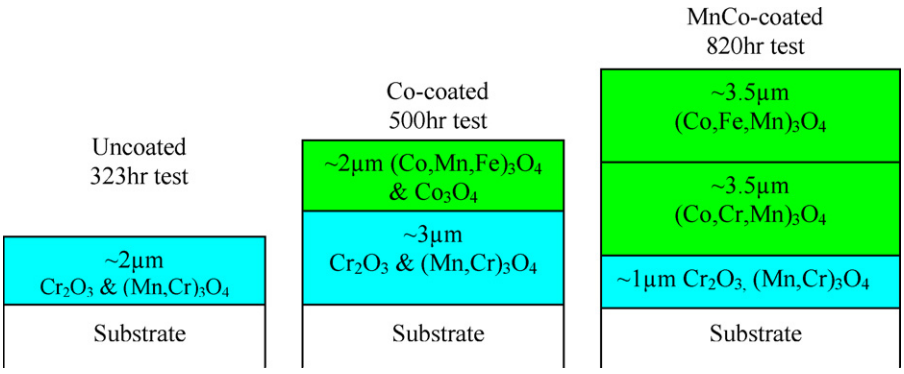

Fig. 9. Schematic structure of oxidation layers after cell test.

top layer and scale layer, a mixed zone is found to be $(Mn,Cr,Co)_3O_4$. Beyond that, no Cr is spotted in the top layer, which means no Cr will poison the SOFC cathode.

Also note that Fe content and scale thickness is higher in cobalt-coated interconnect than MnCo-coated one. Different coating thickness leads to scale growth and element migration difference. No silicon peak is observed at interface (not shown here) due to silicon removal during or after melting.

3.4. XRD patterns of oxidized interconnect surface

XRD patterns of all three interconnects are displayed in Fig. 7. For all three samples, strong Pt peaks and mica peaks are found, which are from Pt paste and the mica gaskets respectively. Only $(Mn,Cr)_3O_4$ and Cr_2O_3 peaks are detected on the surface of uncoated SUS 430. For cobalt-coated interconnect, both $(Co,Mn,Fe)_3O_4$ and Co_3O_4 are detected in the coating layers. Cr_2O_3 and $(Mn,Cr)_2O_4$ phases are also detected, usually from the subscale, but most of the diffraction peaks are assigned to Cr_2O_3, as in prior literatures [23,26]. MnCo-coated interconnect shows strong peaks of $(Mn,Co,Fe)_3O_4$ and a tiny peak of Co_3O_4. Both Cr_2O_3 and substrate peak are barely detectable. Similar results have been reported in long term exposure of slurry painted $(Mn,Co)_3O_4$ coupons. Note there is slight shift of $(Mn,Co,Fe)_3O_4$ peak from cobalt-coated to MnCo-coated interconnect, which is attributable to different composition of these two spinels, as shown by the EDX line scan (Fig. 6).

3.5. Cell cathode

Volatility of Cr containing species, mainly $Cr(OH)_2O_2$ or CrO_3 [1], from the oxidized scale can be reduced at SOFC cathode. This will lead to significant decay of fuel cell power. When using LSM cathodes, Cr species will deposit at the electrolyte and cathode interface to block the triple phase boundary. Fig. 8 shows the cross sections of each tested cell – all the dense bright and gray regions on the left are electrolytes. The interlayers are ~10 μm between electrolyte and cathode. Cr (3 at.%) was detected at the interlayer of Fig. 8(a), thus the microstructure is not as fine as Fig. 8(b). In Fig. 8(c), both the interlayers and cathode shows larger particle size, which might result from the longer test period or two thermal cycles. No Cr was detected in this interlayer.

In summary, during the on-cell tests, both the Co coating and MnCo coating has effectively blocked the Cr evaporation from the substrate materials.

4. Discussion

Cr poisoning has been investigated extensively between various metal and cathode materials. It can be summarized as follows: (1) LSM is more susceptible to Cr poisoning than other cathode materials, such as LSCF and LSF [22,27,28], (2) Cr will evaporate as CrO_3 or $Cr_2(OH)_2O_6$, and then is reduced at the electrochemical active sites, thereby blocking the oxygen reaction sites [1,3,5], and (3) poisonings increases with the amount of polarization as well as the time under current and current density [5,29] via the reactions:

$$2CrO_2(OH)_2(g) + 3Vo^{\bullet\bullet} + 6e^{-1} = Cr_2O_3(g) + 3Oo^{x} + 2H_2O(g) \quad (1)$$

In prior half cell or single cell stack tests, testing had been done at a constant voltage of 0.70 V [22] or constant current of 200 A cm^{-2} [6,24]. The advantage of constant current over constant voltage is obvious: constant current guarantees fuel utilization remains unvaried, even though cell performance may decay with time. This is important, since too high of a fuel utilization can also cause cell degradation [30]. Alternatively, in constant voltage mode (such as 0.7 V), current decay will gradually reduce the rate of Cr species reduction. Accordingly, constant current of 0.75 A was chosen in the present tests, and in the start of each test, the cell voltage at 0.75 A is ~0.70 V to reflect nominal cell operating conditions. As voltage degrades, the constant current is sufficient to reduce the volatile chromium species, thus making this experiment a more stringent test of coating functionality. This approach is also consistent with that proposed by others focused on achieving accurate degradation measurements [31].

The structure of the oxidized coating can be shown schematically, Fig. 9, based on results from XRD and EDX line scans. Cr_2O_3 and $MnCr_2O_4$ are formed on the uncoated SUS 430 surface. Although $MnCr_2O_4$ coverage on the top surface can reduce Cr volatility versus the Cr_2O_3, it is not enough to eliminate it entirely [32]. From the half cell test results of LSM with SUS 430, the cell overvoltage increased sharply with operation time within 100 h [32], and then the decay slows down until the plateau is reached (Fig. 3).

Cobalt-coated SUS 430 displays $(Co,Mn,Fe)_3O_4$ and little Co_3O_4 on the top surface. The scale is ~3 μm thick, which is about 1 μm thicker than the uncoated case. Similar results from Qu et al. [9] shows that a thicker scale layer is formed under a cobalt coating layer (~1 μm) after 500 h test at 750 °C. This result is attributable to initial Fe_2O_3 formation instead of Cr_2O_3. The former is much less dense than the latter. Accordingly, Cr_2O_3 must grow rapidly to form a sufficiently dense scale. Alternatively, for relatively thick cobalt coatings of ~15 [23] and ~80 μm [26], no obvious scale layer is observed. On the other hand, spallation was spotted on ~5 μm Co coating on SUS 430 substrate [33], which occurred between silica and chromia layers. It was suggested that a substrate with low silicon level or with stabilized silicon was preferred to eliminate the spallation and reduce ASR. Though thick cobalt coatings are beneficial to reduce the scale growth, CTE mismatch is another potential threat to the application. Co_3O_4 formed after oxidation has a CTE of 9.3 ppm K^{-1} at 800 °C as reported in [34], and the

other value is ~40 ppm K^{-1} at the same temperature [33]. In spite of four times larger difference, both these numbers will cause CTE mismatch problem. In the present tests, no spallation is evident, even after thermal cycles, which is probably due to the low silicon level of the substrate. Therefore, a critical thickness exists for the pure cobalt-coated interconnects based on low silicon and silicon stabilized substrate.

The MnCo-coated SUS 430 displays a continuous Mn distribution in the coating. A small fraction of Cr is spotted in the middle layer, but none is detected on the top layer, just as reported in the literature [10,12] by Yang et al. The coating layer was mainly composed of $MnCo_2O_4$ with the CTE of ~12 ppm K^{-1}. Additionally, compared with the cobalt-coated case, the scale layer is much thinner (~1 μm). From previous results of ASR testing, only ~1.5 μm scale layer is detected under a ~1.5 μm MnCo coating after 1200 h [20]. Therefore, it can be summarized that both cobalt and MnCo coating can prevent the diffusion of Cr, but addition of Mn into cobalt coating can further suppress the scale growth, and better matches the CTE of the substrate, even if the coating is as thin as 1.5 μm or as thick as 20 μm.

Finally, the cell degradations can be correlated with the cell microstructure, especially the cathode interlayer (Fig. 8). For the cell with the uncoated interconnect, Cr deposited in the interlayer will block the triple phase boundary and significantly increase the polarization resistance, causing rapid degradation [35] The cell with MnCo-coated interconnect shows coarse cathode and interlayer (Fig. 8(b)). It will reduce the triple phase boundary and the diffusion path [36], therefore, degradation will be induced. For the one with the cobalt-coated interconnect, cell cathode interlayer exhibits fine particles with uniform distribution (Fig. 8(c)), so little degradation can be caused.

5. Conclusions

Uncoated, and cobalt and MnCo-coated SUS 430 interconnects were tested with an SOFC for 323, 500 and 820 h, respectively. The results showed that the cell with an uncoated interconnect degrades rapidly in the initial 100 h, then slows down and eventually reach a plateau at ~200 h. Overall, a 33% decay occurred in 320 h. The coated cases show considerable improvements. Degradation rates are estimated at 5% and 9% per 1000 h for cobalt and MnCo-coated interconnects, respectively. Since no Cr is found on the top surface of coating or on SOFC cathode interlayer, the degradation is not attributable to Cr poisoning effect.

Combined with the results from SEM and XRD, the advantages of both coatings are to inhibit Cr diffusion to the top surface. However, the drawbacks of pure cobalt coating are: (1) it accelerates the scale growth for thin coating (~2 μm) and (2) CTE mismatch between top layer Co_3O_4 and substrate can occur for thick coatings. The addition of Mn into cobalt reduces these problems. Scale growth was suppressed significantly the $MnCo_2O_4$ spinel, which improves the conductivity, and the CTE (~12 ppm K^{-1}) closely matches the substrate materials.

Furthermore, the degradation was found to be correlated with the cell cathode interlayer microstructure change. The cell using MnCo-coated interconnect shows coarse interlayer structure, so the degradation is higher compared with the cell with cobalt-coated interconnect.

Acknowledgements

This technical effort was performed in support of the National Energy Technology Laboratory's on-going research in West Virginia University under contract #DE-AC26 -04NT41817. The assistance of Richard Pineault and David Ruehl from NETL in Morgantown, WV, with SOFC testing is acknowledged. The interconnect materials from Dr. Paul Jablonski (NETL Albany), and fruitful discussion with Prof. Harry Finklea (Department of Chemistry, WVU) are also highly appreciated.

References

[1] W.Z. Zhu, S.C. Deevi, Development of Interconnect materials for solid oxide fuel cells, Materials Science & Engineering A 348 (2003) 227–243.
[2] J.W. Fergus, Lanthanum chromite-based materials for solid oxide fuel cell interconnects, Solid State Ionics 171 (2004) 1–15.
[3] J.W. Fergus, Metallic interconnects for solid oxide fuel cells, Materials Science and Engineering A 397 (2005) 271–283.
[4] Z. Yang, K.S. Weil, D.M. Paxton, J.W. Stevenson, Selection and evaluation of heat-resistant alloys for SOFC interconnect applications, Journal of The Electrochemical Society 150 (2003) A1188–A1201.
[5] J.W. Fergus, Effect of cathode and electrolyte transport properties on chromium poisoning in solid oxide fuel cells, International Journal of Hydrogen Energy 32 (2007) 3664–3671.
[6] S.P. Jiang, Y. Zhen, Mechanism of Cr deposition and its application in the development of Cr-tolerant cathodes of solid oxide fuel cells, Solid State Ionics 179 (2008) 1459–1464.
[7] P.D. Jablonski, D.E. Alman, Oxidation resistance and mechanical properties of experimental low coefficient of thermal expansion (CTE) Ni-base alloys, International Journal of Hydrogen Energy 32 (2007) 3705–3712.
[8] M. Stanislowski, J. Froitzheim, L. Niewolak, W.J. Quadakkers, K. Hilpert, T. Markus, L. Singheiser, Reduction of chromium vaporization from SOFC interconnectors by highly effective coatings, Journal of Power Sources 164 (2007) 578–589.
[9] W. Qu, L. Jian, D.G. Ivey, J.M. Hill, Yttrium, cobalt and yttrium/cobalt oxide coatings on ferritic stainless steels for SOFC interconnects, Journal of Power Sources 157 (2006) 335–350.
[10] Z. Yang, G. Xia, G.D. Maupin, J.W. Stevenson, Evaluation of perovskite overlay coatings on ferritic stainless steels for SOFC interconnect applications, Journal of Electrochemical Society 153 (2006) A1852–A1858.
[11] J.-J. Choi, J.-H. Lee, D.-S. Park, B.-D. Hahn, W.-H. Yoon, H.-T. Lin, Oxidation resistance coating of LSM and LSCF on SOFC metallic interconnects by the aerosol deposition process, Journal of American Ceramic Society 90 (2007) 1926–1929.
[12] Z. Yang, G. Xia, S.P. Simner, J.W. Stevenson, Thermal growth and performance of manganese cobaltite spinel protection layers on ferritic stainless steel SOFC interconnects, Journal of Electrochemical Society 152 (2005) A1896.
[13] W. Qu, Li Jian, J.M. Hill, D.G. Ivey, Electrical and microstructural characterization of spinel phases as potential coatings for SOFC metallic interconnects, Journal of Power Sources 153 (2006) 114–124.
[14] D.E. Alman, C.D. Johnson, W.K. Collins, P.D. Jablonski, The effect of cerium surface treated ferritic stainless steel current collectors on the performance of solid oxide fuel cells (SOFC), Journal of Power Sources 168 (2007) 351–355.
[15] Z. Yang, G. Xia, J.W. Stevenson, $Mn_{1.5}Co_{1.5}O_4$ spinel protection layers on ferritic stainless steels for SOFC interconnect applications, Electrochemical and Solid-State Letters 8 (2005) A168.
[16] P.E. Gannon, V.I. Gorokhovsky, M.C. Deibert, R.J. Smith, A. Kayani, P.T. White, S. Sofie, D. Zhenguo Yang, S. McCready, C. Visco, H. Jacobson, Kurokawa, Enabling inexpensive metallic alloys as SOFC interconnects: an investigation into hybrid coating technologies to deposit nanocomposite functional coatings on ferritic stainless steels, International Journal of Hydrogen Energy 32 (2007) 3672–3681.
[17] C. Johnson, R. Gemmen, C. Cross. Alloy Films Deposited by Electroplating as Precursors for Protective Oxide Coatings on Solid Oxide Fuel Cells Metallic Interconnect Materials, MS&T'06 conference, Cincinnati.
[18] M.R. Bateni, P. Wei, X. Deng, A. Petric, Spinel coatings for UNS 430 stainless steel interconnects, Surface and Coatings Technology 201 (2007) 4677–4684.
[19] J. Wu, Y. Jiang, C. Johnson, X. Liu, DC electrodeposition of Mn–Co alloys on stainless steels for SOFC interconnect application, Journal of Power Sources 177 (2008) 376–385.
[20] J. Wu, J. Christopher, J. Yinglu, R.S. Gemmen, L. Xingbo, Pulse plating of Mn-Co alloys for SOFC interconnect applications, Electrochimica Acta 54 (2008) 793–800.
[21] Y.D. Zhen, A.I.Y. Tok, S.P. Jiang, F.Y.C. Boey, La(Ni,Fe)O_3 as a cathode material with high tolerance to chromium poisoning for solid oxide fuel cells, Journal of Power Sources 170 (2007) 61–66.
[22] S.P. Simner, M.D. Anderson, G. Xia, Z. Yang, L.R. Pederson, J.W. Stevenson, SOFC performance with Fe-Cr-Mn alloy interconnect, Journal of Electrochemical Society 152 (2005) A740–A745.
[23] C.D. Johnson, J. Wu, X. Liu, R.S. Gemmen. Solid oxide fuel cell performance using metallic interconnects coated by electroplating methods, Fuel Cell Science, Engineering and Technology Conference, 2007, New York, USA.
[24] K. Fujita, K. Ogasawara, Y. Matsuzaki, T. Sakurai, Prevention of SOFC cathode degradation in contact with Cr-containing alloy, Journal of Power Sources 131 (2004) 261–269.
[25] M.G.E. Cox, B. McEnanay, V.D. Scott, A chemical diffusion model for partitioning of transition elements in oxide scales on alloys, Philosophical Magazine 26 (1972) 839–851.
[26] X. Deng, P. Wei, M.R. Bateni, A. Petric, Cobalt plating of high temperature stainless steel interconnects, Journal of Power Sources 160 (2006) 1225–1229.

[27] S.P. Jiang, S. Zhang, Y.D. Zhen, Deposition of Cr species at (La,Sr)(Co,Fe)$_3$ cathodes of solid oxide fuel cells, Journal of Electrochemical Society 153 (2006) 127–134.
[28] Y. Matsuzaki, I. Yasuda, Dependence of SOFC cathode degradation by chromium-containing alloy on compositions of electrodes and electrolytes, Journal Electrochemical Society 148 (2001) A126.
[29] S.P.S. Badwal, R. Deller, K. Foger, Y. Ramprakash, J.P. Zhang, Interaction between chromia forming alloy interconnects and air electrode of solid oxide fuel cells, Solid State Ionics 99 (1997) 297–310.
[30] R.S. Gemmen, C.D. Johnson, Evaluation of fuel cell system efficiency and degradation at development and during commercialization, Journal of Power Sources 159 (2006) 646–655.
[31] R.S. Gemmen, M.C. Williams, K. Gerdes, Degradation measurement and analysis for cells and stacks, Journal of Power Sources 184 (2008) 251–259.
[32] K. Fujita, T. Hashimoto, K. Ogasawara, H. Kameda, Y. Matsuzaki, T. Sakurai, Relationship between electrochemical properties of SOFC cathode and composition of oxide layer formed on metallic interconnects, Journal of Power Sources 131 (2004) 270–277.
[33] N. Shaigan, D.G. Ivey, W. Chen, Co/$LaCrO_3$ composite coatings for AISI 430 stainless steel solid oxide fuel cell interconnects, Journal of Power Sources 185 (2008) 331–337.
[34] A. Petric, H. Ling, Electrical conductivity and thermal expansion of spinels at elevated temperatures, Journal of American Ceramic Society 90 (2007) 1515–1520.
[35] Y.D. Zhen, J. Li, S.P. Jiang, Oxygen reduction on strontium-doped $LaMnO_3$ cathodes in the absence and presence of an iron–chromium alloy interconnect, Journal of Power Sources 162 (2006) 1043–1052.
[36] H. Yokokawa, H. Tu, B. Iwanschitz, A. Mai, Fundamental mechanisms limiting solid oxide fuel cell durability, Journal of Power Sources 182 (2008) 400–412.